Benzoquinone and naphthoquinone based redox-active labels for electrochemical detection of modified oligonucleotides on Au electrodes

Leonid A. Shundrin, Irina G. Irtegova, Nadezhda V. Vasilieva, Irina A. Khalfina

PII: S0040-4039(15)30450-0
DOI: http://dx.doi.org/10.1016/j.tetlet.2015.12.035
Reference: TETL 47082

To appear in: *Tetrahedron Letters*

Received Date: 10 September 2015
Revised Date: 1 December 2015
Accepted Date: 8 December 2015

Please cite this article as: Shundrin, L.A., Irtegova, I.G., Vasilieva, N.V., Khalfina, I.A., Benzoquinone and naphthoquinone based redox-active labels for electrochemical detection of modified oligonucleotides on Au electrodes, *Tetrahedron Letters* (2015), doi: http://dx.doi.org/10.1016/j.tetlet.2015.12.035

Benzoquinone and naphthoquinone based redox-active labels for electrochemical detection of modified oligonucleotides on Au electrodes

Leave this area blank for abstract

Leonid A. Shundrin, Irina G. Irtegova, Nadezhda V. Vasilieva, Irina A. Khalfina

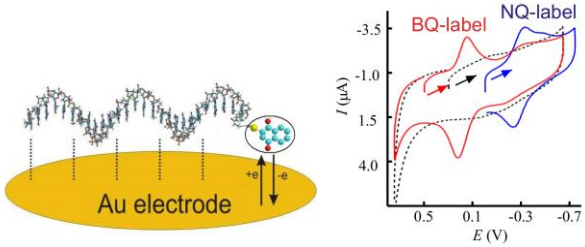

Benzoquinone and naphthoquinone based redox-active labels for electrochemical detection of modified oligonucleotides on Au electrodes

Leonid A. Shundrin[a,b,c*], Irina G. Irtegova[a,b], Nadezhda V. Vasilieva[a], Irina A. Khalfina[a,b]

[a] *N. N. Vorozhtsov Institute of Organic Chemistry, Siberian Branch of the Russian Academy of Sciences, Academician Lavrent'ev Avenue, 9 , 630090 Novosibirsk, Russian Federation*

[b] *Department of Natural Sciences, National Research University – Novosibirsk State University, Pirogova Str. 2, 630090 Novosibirsk, Russian Federation*

[c] *The Scientific Institute of Clinical and Experimental Lymphology, Siberian Branch of the Russian Academy of Medical Sciences, Timakova Str. 4, 630060 Novosibirsk, Russian Federation*

Keywords: quinones; redox-active labels; electrochemical reduction; cyclic voltammetry; modified oligonucleotides

Abstract: The reaction of 1,4-benzoquinone and 1,4-naphthoquinone with β-thiopropionic acid yielded 3-[(3,6-dioxocyclohexa-1,4-diene-1-yl)thio]propionic and 3-[(1,4-dioxo-1,4-dihydronaphthalene-2-yl)thio]propionic acids, respectively. These compounds were used to modify oligonucleotides to allow their electrochemical detection on the surface of Au electrodes using cyclic voltammetry. Electrochemical reduction of the corresponding amides, modeling the bonding of the redox-active labels with molecules that are not electrochemically active, was also studied.

Elaboration of electrochemical DNA biosensors, also known as genosensors, has achieved noticeable progress in the last decade.[1] Methods used for DNA detection on the surface of electrodes can be classified into two main types depending on the nature of the electrochemical signal: label-free and label-based. The former use the signal resulting from hybridization itself[2] while the latter use small electrochemically active molecules, which are inserted into oligonucleotides and ds-DNA fragments (or amplicons) as redox-active labels. These labels must meet strict demands: low redox potentials, chemical stability and reversibility towards electron transfer in water buffers to avoid label decay under potential sweep. The main types of compounds studied as redox-active labels in electrochemical genosensing technologies are based

* Corresponding author. Tel.: +7-383-330-94-32; fax: +7-383-330-97-52; e-mail: shundrin@nioch.nsc.ru

on ferrocene,[3] 9,10-anthraquinone derivatives,[4] transition metals complexes with organic electrochemically active moieties[5] and some types of redox-active intercalators.[6] Several types of organic electrochemically active labels reported to date have close redox potentials, for example, derivatives of 9,10-anthraquinone.[4] Thus, the synthesis of redox-active labels with different and well-discriminated potentials is a vital problem because a set of labels with various redox potentials can be used for simultaneous electrochemical detection of different site-specific DNA fragments in electrochemical microarray technologies. From this point of view the task of synthesising a large number of redox-active labels is similar to the analogous task in fluorescence based microarray analysis, for which a set of fluorescent labels with different spectral properties has been synthesized.[7] The goal of this study was the synthesis and testing of redox-active modifiers of oligonucleotides to allow their electrochemical detection at the surface of Au electrodes using cyclic voltammetry (CV). Well distinguished potentials of the redox active modifiers in their cyclic voltammograms was the main requirement of this study, and the creation of specific genosensing technologies was not considered at this stage.

Naphthoquinone (NQ), benzoquinone (BQ) and their derivatives have low electrochemical reduction potentials, and their electrochemistry has been well studied in various media.[8-11] The stable electrochemical activity of NQ and BQ was exploited for their application in biosensors in recent years. Charge transfer interaction between quinones and melamine was used to determine the latter by voltammetric methods.[12] NQ-based polymers have been applied to design electrochemical immunosensors.[13] Several intracellular nanosensors based on BQ- and NQ-modified nanoparticles were recently proposed for the determination of cell oxidative stress. [14,15] NQ and BQ moieties possess well distinguished potentials in water buffers making them suitable to use as redox-active labels for oligonucleotides.

NQ(BQ)-based modifiers (**1**, **2**) for oligonucleotides were synthesized using *S*-nucleophilic addition of β-thiopropionic acid to the double bond of NQ and BQ followed by aerobic oxidation or using PbO_2 (for details see ESI). To test **1**, **2** as redox active labels, the corresponding amides (**3**, **4**) were synthesised. These compounds model the bonding of **1**, **2** with molecules that are not electrochemically active. Then, the electrochemical reduction (ECR) of **3**, **4** in MeCN and MeCN:H_2O mixtures with variable water content were studied using cyclic voltammetry.[16]

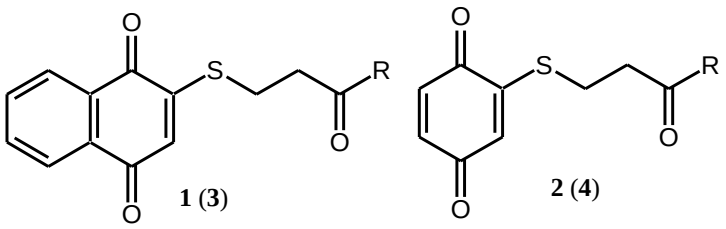

Figure 1. Structures of the compounds. R= OH (**1, 2**); NH*i*Pr (**3, 4**).

The mechanisms of NQ and BQ ECR are known to be different in aprotic solvents and H_2O.[7] ECR of both compounds is an electron-electron (EE) - process in aprotic solvents with the formation of a long-lived radical anion (RA) and dianion (DA), whereas protonation of RA and DA should be taken into account in the aqueous media.[8] Cyclic voltammograms (CV) of **3, 4** in MeCN and its mixtures with H_2O were characterized by two or three (for **3** in MeCN only) diffusion controlled ($I_p^{iC} \cdot \nu^{-1/2}$ = const, where I_p^{iC} is the peak current[17], and ν is the potential sweep rate) reduction peaks (Fig. 3a-d for **3**). The CV of **4** are shown in ESI Fig. S1. The corresponding peak potentials of **3**, **4** (Table 1) become less negative with the increase of the H_2O content in the mixture. The second peak becomes irreversible when the molar fraction of H_2O (m) exceeds 0.1 for **3** and 0.2 for **4,** and in both cases is not observable when m>0.4. The only diffusion controlled and one-electron reversible peak ($\Delta E_p = E_p^{1A} - E_p^{1C} = 0.058$ V) was observed in the CV of both compounds in H_2O (Fig. 3d,f, ESI Fig. S1d). To understand the changes in the CV of **3**, **4** in binary MeCN:H_2O mixtures, we considered a common ECR mechanism, which includes three one-electron electrochemical reactions and three non electrochemical protolytic equilibria where Q is **3** or **4** (Figure 2).

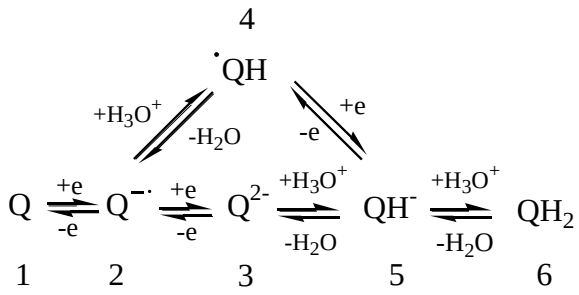

Figure 2. Common ECR mechanism of quinone-type compounds.

Table 1. Experimental reductive peak potentials of compounds **3, 4** in MeCN:H_2O mixtures.

3			**4**		
m	E_p^{1C}, V	E_p^{2C}, V	m	E_p^{1C}, V	E_p^{2C}, V
0[a]	−0.70	−1.19	0	−0.52	−1.11
0.1	−0.59	−0.82	0.1	−0.40	−0.63
0.244	−0.54	−0.69	0.218	−0.34	−0.53
0.301	−0.53	−0.67	0.334	−0.31	−0.50
0.447	−0.51	—	0.456	−0.29	—
0.519	−0.51	—	0.528	−0.27	—
0.921	−0.37	—	0.737	−0.23	—
0.977	−0.33	—	0.808	−0.21	—
1.0	−0.32	—	1.0	−0.13	—

a E_p^{3C} = –1.38 V was observed for **3** only when m=0.

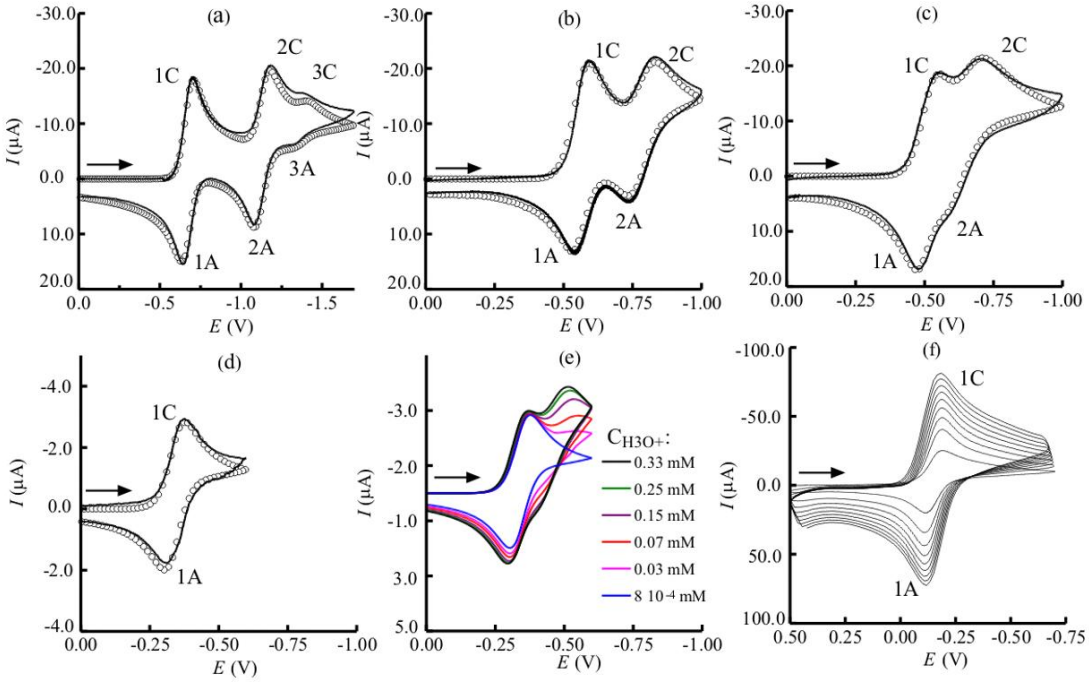

Figure 3. Cyclic voltammograms (solid line) and their simulations (circles) of **3** in MeCN (a), MeCN:H_2O mixtures (m= 0.1 (b), 0.244 (c)), H_2O (d), model CV curves with various H_3O^+ concentrations when the mechanism **III** (Fig. 2) is assumed (e) and CVs of **4** in H_2O at ν=100, 300, 700, 900, 1100, 1300, 1500, 1700, 1900 $mV \cdot s^{-1}$ (f). Arrows indicate the direction of potential sweep.

It is convenient to present possible schemes of mechanisms as graphs. The points of the graphs are molecules involved in the reaction mechanism (1-6), and the edges are one-electron transfer reactions or protolytic equilibria (Fig. 4).

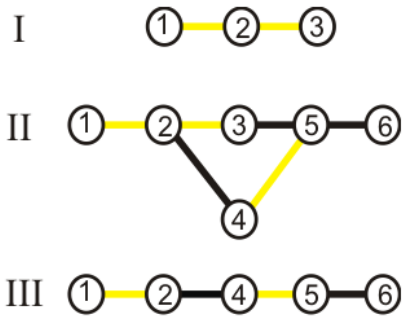

Figure 4. Topological representation of the ECR mechanisms of **3**, **4** in MeCN:H_2O mixtures (yellow edges are one-electron transfer reactions, black edges are protolytic equilibria).

The ECR of **4** in MeCN (ESI Fig. S1) is an example of a classical EE-process (**I** in Fig. 4) with two well-separated one-electron reversible peaks in the CV curve. Meanwhile, the ECR of **3** in MeCN can be adequately simulated[18] only when mechanism **II** is used (Fig. 3a). In accordance with the CV simulation data, the 3C peak corresponds to the ECR of the protonated form of **3** RA.

The EPR spectra of **3, 4** RAs together with their protonated forms were observed under electrochemical reduction of **3, 4** at potential E_p^{1C}. Both spectra were characterized by broadened lines in MeCN due to proton exchange between the oxygen atoms of the quinone moieties. This exchange became fast in H_2O leading to line narrowing (ESI Fig. S2).

The increase of the water content in the MeCN:H_2O mixture results in a decrease of the heterogeneous electron transfer constants at the second electrochemical stage, whereas the first stage remained reversible over the whole range of m (ESI Table S1). In accordance with the CV simulation data, the ECR mechanism changes as follows: **II** (m=0)→**III**(m>0) for **3** (Fig. 3a-d) and **I** (m=0)→**II** (m~0.1)→**III**(m>0.1) for **4** (ESI Fig. S1). To understand why only one reversible one-electron peak was observed in the CVs of **3**, **4** in H_2O (Fig. 3d, ESI Fig. S1), we considered a model simulation of the CV of **3** at different H_3O^+ concentrations (Fig. 3e) using mechanism **III** (Fig. 4). The decrease in the H_3O^+ concentration from 0.25 mM to 0.001 mM (pH of the aqueous solution was 6.2 under experimental conditions) resulted in a decrease of the protonated **3** RA concentration (particle 4 in graph **III**). In turn, this was accompanied by the decrease of I_p^{2C}, corresponding to one-electron transfer to particle 4. As a result, the second electrochemical stage became not observable. The corresponding CV in this case has a one-electron reversible diffusion-controlled peak, which was dependent on the potential sweep rate as $\nu^{0.5}$ (Fig. 3f , ESI Fig. S1a, example for **4**). The situation is reversed if the ECR mechanism, including DA formation is accepted. In this case, the I_p^{2C} decrease was not observed when the

H_3O^+ concentration is decreased. This proves that only mechanism **III** is correct for an adequate description of the ECR of **3**, **4** in H_2O. Note, that the ECR of **3**, **4** in 50 mM phosphate buffer at pH 7.2 using an Au disk electrode gave the same results. When the Au electrode was used, the peak potentials of the ECR of **3**, **4** were equal to –0.34 and +0.10 V, respectively.

In accordance with literature data,[8,14] quinoid substances in general undergo two-electron ECR in aqueous buffers. Contrary to this, we showed that the ECR of **3**, **4** in H_2O at pH 6.2-7.2 was in fact a one-electron reversible process. The transfer of the second electron was not observed due to the kinetic reasons. This meant that the corresponding acids **1**, **2** could be used as redox-active modifiers of oligonucleotides without limitation in potential sweep, because no irreversible processes accompanying the loss of the label electrochemical activity are observed.

To test acids **1**, **2** as redox-active labels in the model oligonucleotide structures, the modified oligonucleotides were prepared by modification of the corresponding amino-terminated 27-base oligonucleotide via *N*-succinimide derivatives of **1**, **2**:

NQ(BQ)–S–$(CH_2)_2$–C(O)NH–$(CH_2)_6$–5'-TTGGCAGAAGCTATGAAACGATATGGG-3'

(for oligonucleotide synthesis and modification see ESI). The base sequence of the model oligonucleotide was identical to the sequence of the quality control oligo probe (QC) which was used in the microarray analysis. [19] Labeled QC was purified by reprecipitation from ethanol followed by gel-filtration using Sephadex G-25 gel column chromatography. The final concentration of the labeled QC was adjusted to 100 μM.

A specially designed thin-layer electrochemical cell with three working electrodes equipped with a manual switch between the working electrodes was used in the experiments. An Ag disk electrode was used as a reference electrode. A standard microscope glass with 200 Å Au sputtering served as an auxiliary electrode (ESI Fig. S3a,b). The working electrode surface was prepared in accordance with a described previously procedure [20,21] (ESI). After purification of the working electrode surface, the electrochemical cell was dried in an Ar flow. Then, 5 μl of a 100 μM solution of BQ- and NQ-labeled QC were dropped onto the surface of the working electrodes (electrode 1 and 2, respectively, ESI Fig. S3b) followed by drying overnight in air. A solution of unmodified QC was dropped onto electrode 3 for comparison. To remove any unadsorbed oligonucleotide, the cell was washed twice for 3 min in 50 mM phosphate buffer (pH=7.2). Then, 1.2 ml of the buffer was added into the cell electrode cavity and covered by the auxiliary electrode (ESI Fig. S3c). CV were sequentially measured at each electrode using the manual switch between the electrodes. CV are shown in the overlay mode (Fig. 5) and contain redox peaks corresponding to the electrochemical responses from the QC labeled with BQ

(electrode 1) and NQ (electrode 2), whose potentials were sufficiently different to identify the type of the label. No electrochemical signal from the unlabeled QC was detected.

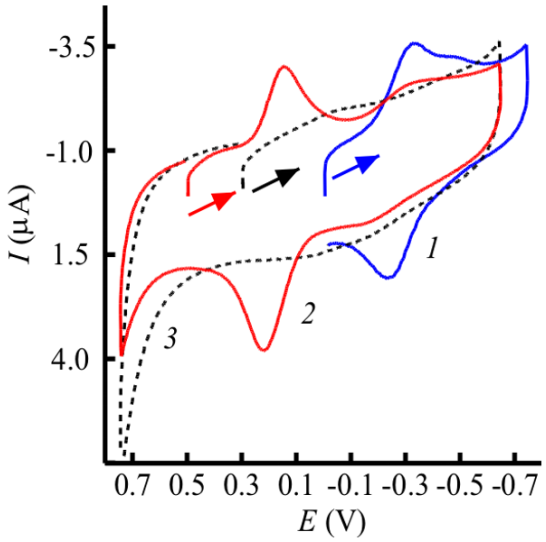

Figure 5. CV scans of the working electrodes of the thin-layer electrochemical cell with adsorbed QC oligonucleotides labeled with NQ (*1* – electrode 1), BQ (*2*- electrode 2) and without a label (*3* – electrode 3). (50 mM phosphate buffer, the initial delay in potential sweep was 5 s, ν=0.1 $V \cdot s^{-1}$, arrows indicate the beginning and direction of the potential sweep).

The sensor electrodes modified with the labeled oligonucleotides were quite stable and displayed electrochemical activity for at least two weeks when stored under an inert atmosphere. The redox signal from both labeled oligonucleotides could be observed over 80-90 potential sweep cycles.

Thus, we report the synthesis and electrochemical properties of benzoquinone and naphthoquinone based redox-active modifiers of oligonucleotides, which make electrochemical detection of oligonucleotides on the surface of Au electrodes possible. The mechanism study of the label electrochemical reduction demonstrated the one-electron and reversible nature of the first step of their ECR in H_2O and phosphate buffer with pH=7.2. Other electrochemical processes resulting in the loss of the labels electrochemical activity were not observed under the studied experimental conditions. Both labels were stable in the oligonucleotide structure and gave quite steady electrochemical signals after adsorption of the labeled oligonucleotides onto Au electrodes. The elaborated labels possess well-distinguished ECR potentials, the values of which fall into “free” potential area between the potentials of anthraquinone and ferrocene based redox-active labels[4] and can be used in electrochemical genosensing technologies, for which the simultaneous use of a number of labels with different redox potentials is required.

Acknowledgments

We are grateful to the Russian Federation Ministry of Education and Science for support within the Project of Joint Laboratories of the Siberian Branch of the Russian Academy of Sciences and National Research Universities.

References

1. Tosar, J. P.; Branas, G.; Laiz, J. *Biosens. Bioelectron.* **2010**, 26, 1205.

2. Caruso, F.; Rodda, E.; Furlong D. N. *Anal. Chem.* **1997**, 69, 2043.

3 Anne, A.; Bouchardon, A.; Moiroux, J. *J. Am. Chem. Soc*. **2003**, 125, 1112.

4 Di Giusto, D. A.; Wlassoff, W. A.; Giesebrecht, S.; Gooding, J. J.; King G. C. *J. Am. Chem. Soc*. **2004**, 126, 4120.

5 Gao, Z.; Yu, Y. H. *Biosens. Bioelectron*. **2007**, 22 (6), 933.

6 Tansil, N. C.; Xie, F.; Xie, H.; Gao, Z. *Chem. Commun*. **2005**, 8, 1064.

7 Shena M. *Microarray Analysis*. Ed.; John Whiley & Sons, Inc.: Hoboken, New Jersey, 2003, pp 1-664.

8 Guin, P. S.; Das, S.; Mandal P.C. *Intern. J. Electrochem.* **2011**, 2011, 1-22.

9 Soriaga, M. P.; Wilson, P. H.; Hubbard, A. T.; Benton, C. S. *J. Electroanal. Chem.* **1982**, 142, 317.

10 He, P.; Crooks, R. M.; Faulkner, L. R. *J. Phys. Chem.* **1990**, 94, 1135.

11 Ji, X.; Banks, C. E.; Silvester, D. S.; Wain, A. J.; Compton R. G. *J. Phys. Chem. C* **2007**, 111, 1496.

12 Zhang, L.; Li, T.; Yu, P.; Ohsaka, T.; Mao, L.; *Electrochem. Comm.* **2013**, 26, 89.

13 Piro, B.; Reisberg, S.; Anquetin, G.; Duc, H.-T.; Pham, M.-C. *Biosensors.* **2013**, 3, 58.

14 Thomson, P. I. T.; Camus, V. L.; Hu, Y.; Campbell, C. J. *Anal. Chem.* **2015**, 87(9), 4719.

15 Jiang, J.; Auchinvole, C.; Fisher, K.; Campbell, C. J. *Nanoscale*. **2014**, 6, 12104.

16 Details of CV experiments, the electrochemical and kinetic parameters for CV simulations are described in Electronic Supplementary Information (ESI).

17 *i* is a number of peaks, symbols “A” or “C” indicate the anode or cathode branch of the CV curve. The designation of potentials is the same.

18 CV simulations were performed using electrochemical simulation package (ESP, v.2.4) designed by Carlo Nervi, Università di Torino, Italy. A simplex algorithm was used for multiparametric optimization implemented in the package.

19 Ryabinin, V. A.; Shundrin, L. A.; Kostina, E. V.; Laassri, M.; Chizhikov V.; Shchelkunov, S. N.; Chumakov, K.; Sinyakov, A. N. *Journal of Medical Virology*, **2006**, 78, 1325.

20 Pang D.-W.; Abruña H. D. *Anal. Chem*., **1998**, 70, 3162.

21 Pang D.-W.; Abruña H. D. *Anal. Chem*., **2000**, 72, 4700.